FDTD Implementations of Integrated Dependent Sources in Full-Wave Electromagnetic Simulations

Khaled ElMahgoub [1,2] and Atef Z. Elsherbeni [3]

[1] Trimble Navigation, Woburn, MA 01801, USA
kelmahgoub@ieee.org

[2] Auto-ID Labs
Massachusetts Institute of Technology, Cambridge, MA 02139, USA

[3] Electrical Engineering and Computer Science Department
Colorado School of Mines, Golden, CO 80401, USA
aelsherb@mines.edu

Abstract ─ The implementation of dependent sources such as: Current Controlled Current Source in full-wave electromagnetic simulation using the Finite-Difference Time-Domain method is introduced. This simple new approach is verified with several numerical examples. In one example, the CCCS is used to implement a circuit with Bipolar Junction Transistor. Good agreement is obtained when the results of the developed FDTD code are compared with those based on analytical solution.

Index Terms ─ Bipolar Junction Transistor (BJT), Current Controlled Current Source (CCCS), Current Controlled Voltage Source (CCVS), dependent sources, Finite-Difference Time-Domain (FDTD), Voltage Controlled Current Source (VCCS), Voltage Controlled Voltage Source (VCVS).

I. INTRODUCTION

The Finite-Difference Time-Domain (FDTD) method has gained great popularity as a tool for full wave electromagnetic simulations. Although it is based on a time-domain solution, it provides a wideband frequency-domain response using time to frequency transformation. It can easily handle composite geometries consisting of different types of materials. In addition, it can easily implement different algorithms for parallel computations. These features of the FDTD have made it one of the most attractive techniques in computational electromagnetics for many applications [1]-[2]. One of the strengths of the FDTD method is implementation of lumped linear and nonlinear circuit elements such as resistors, inductors, capacitors, diodes, transistors, etc. In addition, it can implement independent sources such as current and voltage sources which makes FDTD method widely used in simulating microwave circuits, such as amplifiers, active filters, etc. These circuits usually consist of nonlinear components as well as linear components. Most of the nonlinear elements such as transistors are modeled using dependent sources. A dependent source is a source that generates a voltage or current whose value depends on another voltage or current in the same circuit. There are in general four different types of dependent sources, namely: Voltage Controlled Current Source (VCCS), Current Controlled Current Source (CCCS), Voltage Controlled Voltage Source (VCVS) and Current Controlled Voltage Source (CCVS). Dependent sources appear in most of the equivalent circuit models for devices such as: Bipolar Junction Transistor (BJT) and Metal Oxide Field Effect Transistor (MOSFET), operational amplifiers, static substrate thermal coupling, etc.

To the best of the authors' knowledge, the full implementation of dependent sources using FDTD has not been adequately addressed before, except in [3]-[5], which doesn't cover all four kinds of

dependent sources. One should point out, that the direct implementation of nonlinear devices such as transistors in full wave simulation using FDTD, has been previously investigated by many research groups [6]-[17]. For example, the work done in [6], where Ebers-Moll model was used to implement BJT using Newton Raphson method; in [7] and [8], the BJT was implemented by applying Taylor expansion on the nonlinear transport equations of the BJT based on Gummel-Poon model; while in [10], FDTD formulation based on two port network formulation using its admittance matrix and then transformed to Z-domain and then to difference equation is used to model such devices. In [11], a coupled FDTD-SPICE is used to implement an amplifier, [12] describes a voltage-source-based formulation for the purpose of modeling microwave devices, [13] applies the extended FDTD method to implement nonlinear active microwave circuits. In [14] and [15], reduced nonlinear lumped network FDTD method for the global modeling of RF and microwave circuits is presented. While in [17], 2-D FDTD extended method is used to implement non-linear elements.

In this paper, simple implementation of all four kinds of dependent sources using FDTD is introduced with efficient use of both memory and computational time. This new approach can be used to analyze circuits containing VCCS, CCCS, VCVS and CCVS, or circuits with devices such as MOSFETs, BJTs, operational amplifier or any kind of devices that can be represented using dependent sources in their equivalent circuit model. The FDTD updating equations of the different dependent sources will be derived and used directly to simulate several resistive circuits with different dependent sources. In addition, these dependent sources will be used to represent non-linear devices such as BJT with its equivalent model as an application for the dependent sources implementation. The paper is organized as follows: in Section II, the dependent sources implementation approach is described and the FDTD equations are derived. In Section III, numerical examples to prove the validity of the new approach are presented, including a simple resistive circuits with different dependent sources, and BJT circuit. In Section IV, conclusions are provided.

II. FDTD IMPLEMENTATION

In this section, the new approach is described

and the FDTD updating equations are derived. In general, every dependent source is connected between two adjacent nodes and its value is controlled by the voltage or the current between two other nodes that are not necessary adjacent to each other. To drive the FDTD updating equations for different dependent sources, let's consider the four circuits shown in Figs. 1 (a), (b), (c) and (d). As shown in the figure, all nodes can be normally updated using lumped elements FDTD implementation as in [1], except for the dependent source which needs special handling. For all nodes containing dependent sources, the current density J_{iz} needs to be represented in terms of the controlling parameter voltage (V_0) or current (I_0) as shown in Fig. 1.
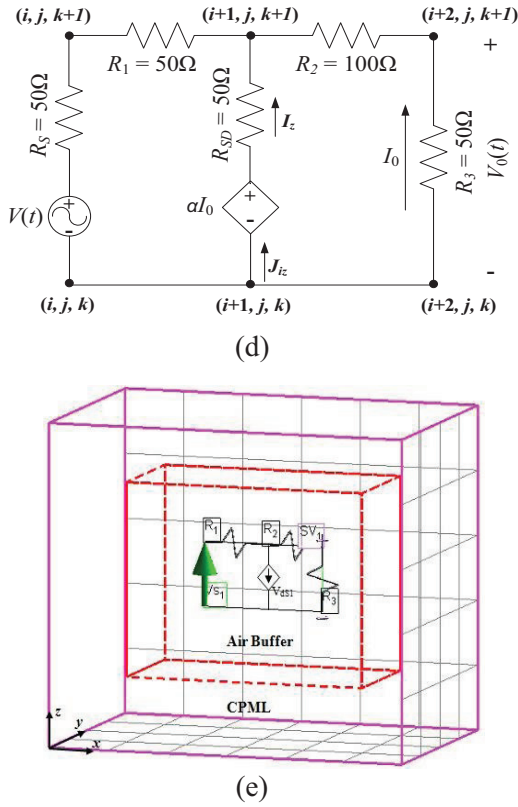

(a)

(b)

(c)

(d)

(e)
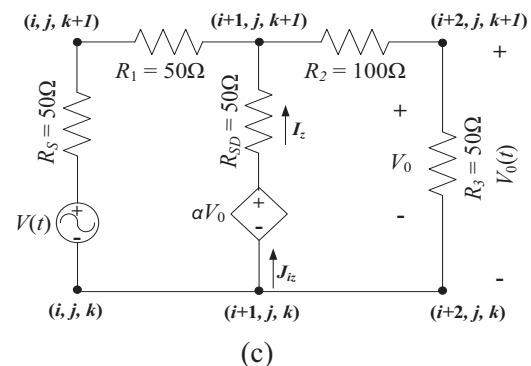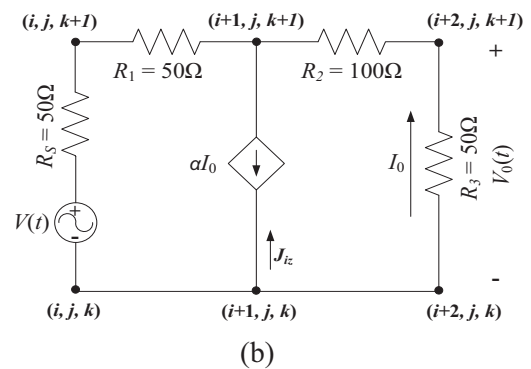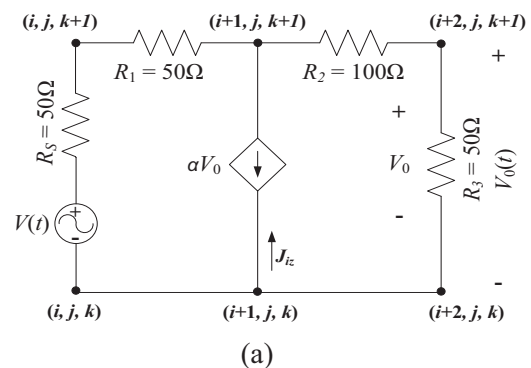
Fig. 1. Simple resistive circuits with different kinds of dependent sources: (a) VCCS, (b) CCCS, (c) VCVS, (d) CCVS, and (e) FDTD computational domain for circuit (a).

The controlling voltages and currents can be calculated using the same formulas used for the sampled current and voltages as presented in [1]. For example, for elements oriented along the z-direction and connected between two nodes with the k index ranges from s to e, we get for the sampled voltage:

$$V_{ZSampled} = -\int \vec{E} \cdot \vec{dl}, \tag{1}$$

writing (1) in discrete form:

$$
V_{ZSampled}^{n+\frac{1}{2}} = -\Delta z \times \sum_{k=ks}^{ke-1} E_Z^{n+\frac{1}{2}}(is, js, k)
$$
$$
= -\Delta z \times \sum_{k=ks}^{ke-1} \left[\frac{E_Z^{n+1}(is, js, k) + E_Z^n(is, js, k)}{2} \right], \tag{2}
$$

and for the sampled currents between the same two nodes, one has:

$$I_{ZSampled} = \oint \vec{H} \cdot \vec{dl}, \tag{3}$$

writing (3) in discrete form:

$$
I_{Zsampled}^{n+\frac{1}{2}} = \Delta x \times \sum_{i=is}^{ie} H_x^{n+\frac{1}{2}}(i, js-1, ke-1)
$$
$$
+ \Delta y \times \sum_{j=js}^{je} H_y^{n+\frac{1}{2}}(ie, j, ke-1)
$$
$$
- \Delta x \times \sum_{i=is}^{ie} H_x^{n+\frac{1}{2}}(i, je, ke-1)
$$
$$
- \Delta y \times \sum_{j=js}^{je} H_y^{n+\frac{1}{2}}(is-1, j, ke-1), \tag{4}
$$

where is, ie, js, je, ks and ke are the minimum and maximum cell indices in x, y, and z-direction, respectively. In this implementation the sampled voltage or current is used directly as the controlling value instead of calculating it separately as in [2].

A. VCCS updating equation

To update the electric field at node $(i+1, j, k)$ shown in Fig. 1 (a), the J_{iz} should be calculated as follows:

$$\frac{\partial E_z}{\partial t} = \frac{1}{\varepsilon_z}\left(\frac{\partial H_y}{\partial x} - \frac{\partial H_x}{\partial y} - \sigma_z^e E_z - J_{iz}\right), \tag{5a}$$

where

$$J_{iz}^{n+\frac{1}{2}}(i+1, j, k) = \frac{I_{iz}^{n+\frac{1}{2}}(i+1, j, k)}{\Delta x \Delta y} = \frac{-\alpha V_0^{n+\frac{1}{2}}}{\Delta x \Delta y}, \tag{5b}$$

where n represent the time index, ε is the permittivity of the medium, σ is the conductivity, α is the control factor, and V_0 is equal to $V_{ZSampled}$ between the two nodes $(i+2, j, k)$ and $(i+2, j, k+1)$ at time index $n+\frac{1}{2}$ which can be calculated using (2). The updating equation for E_z^{n+1} at node $(i+1, j, k)$ can then be written using the coefficient convention presented in [1] as follows:

$$
E_z^{n+1}(i+1, j, k) = C_{eze}(i+1, j, k)E_z^n(i+1, j, k)
$$
$$
+ C_{ezhy}(i+1, j, k)\left[H_y^{n+\frac{1}{2}}(i+1, j, k) - H_y^{n+\frac{1}{2}}(i, j, k)\right]
$$
$$
+ C_{ezhx}(i+1, j, k)\left[H_x^{n+\frac{1}{2}}(i+1, j, k) - H_x^{n+\frac{1}{2}}(i+1, j-1, k)\right] \tag{6}
$$
$$
+ C_{ezvccs}(i+1, j, k)V_{ZSampled}^{n+\frac{1}{2}},
$$

where

$$C_{eze}(i+1,j,k) = \frac{A_0}{B_0}, C_{ezhy}(i+1,j,k) = \frac{2\Delta t}{B_0 \Delta x},$$

$$C_{ezhx}(i+1,j,k) = \frac{-2\Delta t}{B_0 \Delta y}, C_{ezvccs}(i+1,j,k) = \frac{2\Delta t\alpha}{B_0 \Delta x \Delta y},$$

$$A_0 = [2\varepsilon_z(i+1,j,k) - \Delta t\sigma_z^e(i+1,j,k)],$$

$$B_0 = [2\varepsilon_z(i+1,j,k) + \Delta t\sigma_z^e(i+1,j,k)]. \tag{7}$$

Using (6), the electric fields at step $n+1$ appear on both sides of the equation due to the use of equation (2). Special sequence for the update of E_z^{n+1} is followed to overcome this issue as explained in section E below.

B. CCCS updating equation

To update the electric field component E_z^{n+1} at node $(i+1,j,k)$ shown in Fig. 1 (b), the J_{iz} should be calculated as follows:

$$J_{iz}^{n+\frac{1}{2}}(i+1,j,k) = \frac{I_{iz}^{n+\frac{1}{2}}(i+1,j,k)}{\Delta x \Delta y} = \frac{-\alpha I_0^{n+\frac{1}{2}}}{\Delta x \Delta y}, \tag{8}$$

where α is the control factor and I_0 is equal to $I_{ZSampled}$ between the two nodes $(i+2,j,k)$ and $(i+2, j, k+1)$ at time index $n+\frac{1}{2}$ which can be calculated using (4). The updating equation at node $(i+1,j,k)$ can then be written using the coefficient convention presented in [1] as follows:

$$E_z^{n+1}(i+1,j,k) = C_{eze}(i+1,j,k)E_z^n(i+1,j,k)$$

$$+C_{ezhy}(i+1,j,k)\left[H_y^{n+\frac{1}{2}}(i+1,j,k) - H_y^{n+\frac{1}{2}}(i,j,k)\right]$$

$$+C_{ezhx}(i+1,j,k)\left[H_x^{n+\frac{1}{2}}(i+1,j,k) - H_x^{n+\frac{1}{2}}(i+1,j-1,k)\right] \tag{9}$$

$$+C_{ezccs}(i+1,j,k)I_{ZSampled}^{n+\frac{1}{2}},$$

with

$$C_{eze}(i+1,j,k) = \frac{A_0}{B_0}, C_{ezhy}(i+1,j,k) = \frac{2\Delta t}{B_0 \Delta x},$$

$$C_{ezhx}(i+1,j,k) = \frac{-2\Delta t}{B_0 \Delta y}, C_{ezvccs}(i+1,j,k) = \frac{2\Delta t\alpha}{B_0 \Delta x \Delta y},$$

where A_0 and B_0 are given by (7). Using (9), the updating equation of the electric field associated with a CCCS can be easily implemented in a FDTD code.

C. VCVS updating equation

The voltage source here is considered as a soft source (with internal resistance R_{SD}). To update the electric field component E_z^{n+1} at the node $(i+1, j, k)$ shown in Fig. 1 (c), the J_{iz} should be calculated as follows:

$$J_{iz}^{n+\frac{1}{2}}(i+1,j,k) =$$

$$\frac{\Delta z}{2\Delta x \Delta y R_{SD}} \times [E_z^{n+1}(i+1,j,k) + E_z^n(i+1,j,k)] \tag{10}$$

$$+\frac{1}{\Delta x \Delta y R_{SD}} \times \alpha V_0^{n+\frac{1}{2}},$$

where α is the control factor and V_0 is equal to $V_{ZSampled}$ between the two nodes $(i+2, j, k)$ and $(i+2, j, k+1)$ at the time index $n+\frac{1}{2}$ which can be calculated using (2). The updating equation at node $(i+1, j, k)$ can then be written using the coefficient convention presented in [1] as follows:

$$E_z^{n+1}(i+1,j,k) = C_{eze}(i+1,j,k)E_z^n(i+1,j,k)$$

$$+C_{ezhy}(i+1,j,k)\left[H_y^{n+\frac{1}{2}}(i+1,j,k) - H_y^{n+\frac{1}{2}}(i,j,k)\right]$$

$$+C_{ezhx}(i+1,j,k)\left[H_x^{n+\frac{1}{2}}(i+1,j,k) - H_x^{n+\frac{1}{2}}(i+1,j-1,k)\right] \tag{11}$$

$$+C_{ezvcvs}(i+1,j,k)V_{Sampled}^{n+\frac{1}{2}},$$

with

$$C_{eze}(i+1,j,k) = \frac{R_{SD}\Delta x \Delta y A_0 - \Delta t\Delta z}{R_{SD}\Delta x \Delta y B_0 + \Delta t\Delta z},$$

$$C_{ezhy}(i+1,j,k) = \frac{2R_{SD}\Delta y\Delta t}{R_{SD}\Delta x \Delta y B_0 + \Delta t\Delta z},$$

$$C_{ezhx}(i+1,j,k) = \frac{-2R_{SD}\Delta x\Delta t}{R_{SD}\Delta x \Delta y B_0 + \Delta t\Delta z},$$

$$C_{ezvcvs}(i+1,j,k) = \frac{-2\Delta t\alpha}{R_{SD}\Delta x \Delta y B_0 + \Delta t\Delta z},$$

where A_0 and B_0 are given by (7). Using (11), the updating equation of the electric field associated with a VCVS can be easily implemented in the FDTD method. For hard voltage sources one can simply set R_{SD} to zero.

D. CCVS updating equation

Similar to the VCVS, the electric field

component E_z^{n+1} at node $(i+1, j, k)$ shown in Fig. 1 (d), can be updated as follows:

$$J_{iz}^{n+\frac{1}{2}}(i+1,j,k) =$$

$$\frac{\Delta z}{2\Delta x \Delta y R_{SD}} \times [E_z^{n+1}(i+1,j,k) + E_z^n(i+1,j,k)] \quad (12)$$

$$+ \frac{1}{\Delta x \Delta y R_{SD}} \times \alpha I_0^{n+\frac{1}{2}},$$

where α is the control factor and I_0 is equal to $I_{ZSampled}$ which can be calculated using (4).

$$E_z^{n+1}(i+1,j,k) = C_{eze}(i+1,j,k)E_z^n(i+1,j,k)$$

$$+ C_{ezhy}(i+1,j,k)\left[H_y^{n+\frac{1}{2}}(i+1,j,k) - H_y^{n+\frac{1}{2}}(i,j,k)\right]$$

$$+ C_{ezhx}(i+1,j,k)\left[H_x^{n+\frac{1}{2}}(i+1,j,k) - H_x^{n+\frac{1}{2}}(i+1,j-1,k)\right] \quad (13)$$

$$+ C_{ezccvs}(i+1,j,k)I_{sampled}^{n+\frac{1}{2}},$$

with

$$C_{eze}(i+1,j,k) = \frac{R_{SD}\Delta x \Delta y A_0 - \Delta t \Delta z}{R_{SD}\Delta x \Delta y B_0 + \Delta t \Delta z},$$

$$C_{ezhy}(i+1,j,k) = \frac{2R_{SD}\Delta y \Delta t}{R_{SD}\Delta x \Delta y B_0 + \Delta t \Delta z},$$

$$C_{ezhx}(i+1,j,k) = \frac{-2R_{SD}\Delta x \Delta t}{R_{SD}\Delta x \Delta y B_0 + \Delta t \Delta z},$$

$$C_{ezccvs}(i+1,j,k) = \frac{-2\Delta t \alpha}{R_{SD}\Delta x \Delta y B_0 + \Delta t \Delta z},$$

while A_0 and B_0 are given by (7). Using (13), the updating equation of the electric field associated with a CCVS can be easily implemented in the FDTD method. For hard voltage sources one can simply set R_{SD} to zero.

E. Updating procedure

Similarly, the procedures can be used for electric field components in x- or y-directions if the dependent sources are along the x- or y-directions. It is necessary to point out that the current implementation allows for easy update for dependent source, close examination of equations (6) and (11) reveals that there is a future field component in the last term of the R.H.S. This term is not considered at the same step as the traditional

FDTD updating sequence. The FDTD approaches for these two equations could be summarized as follows:

1. Update all magnetic field components at time instant $(n+\frac{1}{2})\,\Delta t$ using traditional updating equations [1].
2. Update all electric field components at time instant $(n+1)\,\Delta t$, taking into account the independent sources and lumped elements using traditional updating equations [1], and dependent source using equations (6), (9), (11) and (13). However, for equations (6) and (11), the last term should not be considered at this step.
3. Compute the $V_{ZSampled}$ using (2) then complete the update of (6) and (11) to include the last term in these two equations.
4. Apply the boundary conditions.
5. Increment the time step, n to n+1. Repeat steps 1 to 4.

Step 2 and 3 in the updating sequence above are the key for a successful implementation of this simple and direct implementation of dependent sources in FDTD.

III. NUMERICAL RESULTS

In this section, numerical results generated using the new approach are presented. The FDTD code was developed in MATLAB [18] and run on a computer with an Intel Core i7 CPU Q720, 1.6 GHz with 6 GB RAM. These results demonstrate the validity of the new approach for analyzing circuits with different dependent sources in FDTD. The first set of examples is a simple resistive circuit containing VCCS, CCCS, VCVS or CCVS. The second example is a BJT circuit analyzed using the equivalent circuit model of the BJT. The results are compared with those obtained from analytical solutions.

A. Test case 1 (simple resistive circuits with different dependent sources)

For the circuits shown in Figs. 1 (a), (b), (c) and (d). The FDTD grid cell size is $\Delta x = \Delta y = \Delta z = 0.25$ mm, $\Delta t = 0.43$ psec with 3000 time steps, the circuit is simulated with $3\times1\times2$ cells in x, y and z-directions, respectively, as shown in Fig. 1 (e). Only 8 convolutional perfect matched layers (CPML) are used as the absorbing boundary of the computational domain as implemented in [1], with 5 cells air buffer in every direction. The voltage

source $V(t)$ is implemented using sinusoidal waveform with amplitude of 10 volts and frequency of 5 GHz, the α factor is equal to 0.01 for the circuit in Fig. 1 (a). As for the circuit shown in Fig. 1 (b), $V(t)$ is implemented using a unit step function with amplitude of 5 volts and α factor of 0.1. For the circuit shown in Fig. 1 (c), $V(t)$ is implemented using Gaussian pulse with amplitude of 10 volts and α factor of 0.2. For the circuit shown in Fig. 1 (d), $V(t)$ is implemented using a cosine modulate Gaussian pulse centered at 16 GHz with bandwidth of 8 GHz (in this paper the bandwidth of the modulated Gaussian pulse is defined as the frequency band where the magnitude in the frequency domain reaches 10% of its maximum), amplitude of 20 volts and α of 0.3. The main goal is to implement the circuits with their VCCS, CCCS, VCVS and CCVS using the new approach and calculate the value of the output voltage $V_0(t)$. The results are compared with analytical results in Figs. 2 (a), (b), (c) and (d). The analytical solution is based on mesh analysis method and it was found that for the values of α factors mentioned above: $V_0(t)$ for Fig. 1 (a) is equal to $V(t)/6$, $V_0(t)$ for Fig. 1 (b) it is equal to $0.2083 \times V(t)$, $V_0(t)$ for Fig. 1 (c) is equal to $0.0943 \times V(t)$ and $V_0(t)$ for Fig. 1 (d) is equal to $0.0908 \times V(t)$. Figure 2 demonstrates good agreement between analytical solutions and the results based on the new approach. The computational time is 0.75 minute and the memory usage is 320 KB.
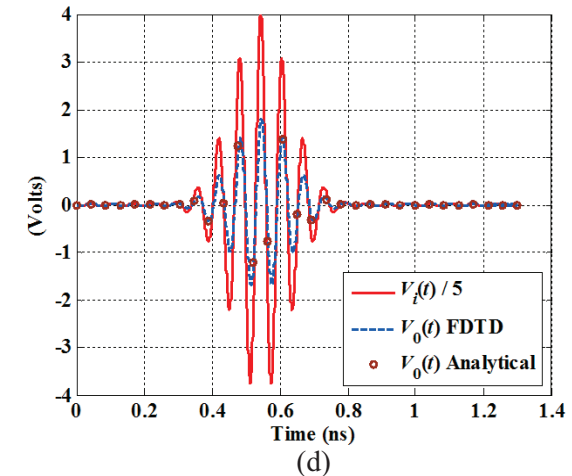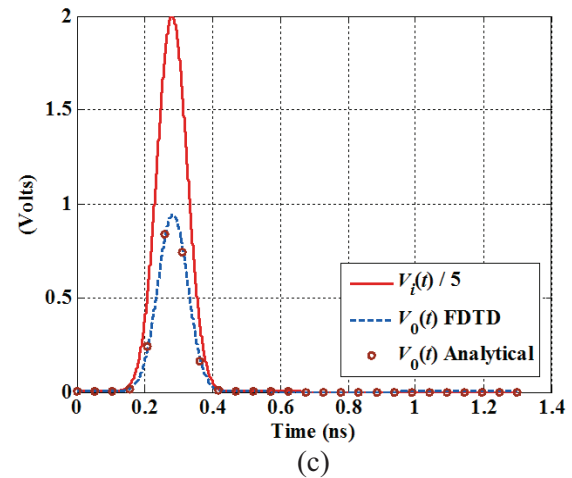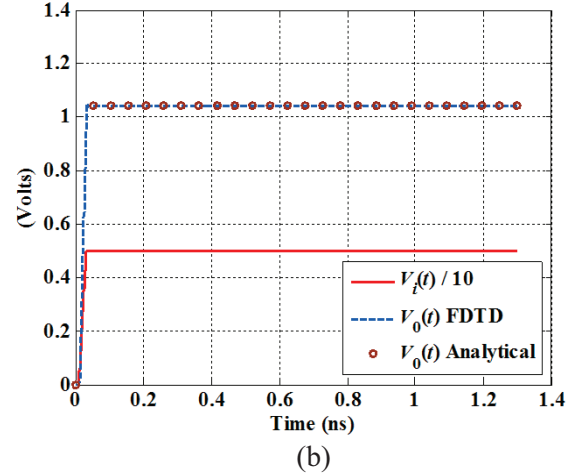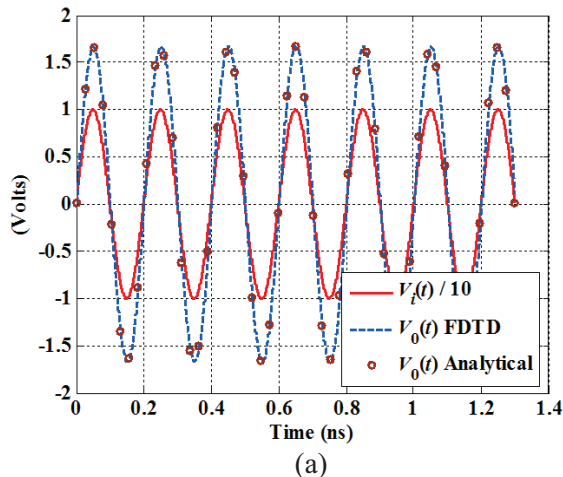

(a)

(b)

(c)

(d)

Fig. 2. Time-domain response for test case 1: (a) VCCS, (b) CCCS, (c) VCVS, and (d) CCVS.

B. Test case 2 (BJT circuit)

In this example, the BJT circuit shown in Fig. 3 (a) is analyzed. It consists of a PNP BJT, two resistor R_C (collector resistor) and R_E (emitter resistor), two infinite capacitors to separate the direct current (DC) biasing from the alternating current (AC), and an input AC voltage source $v_i(t)$. The BJT is implemented in the FDTD using the equivalent circuit model shown in Fig. 3 (b). The values of the equivalent circuit parameters after DC analysis of the circuit according to [19] were found to be $r_e = 27\ \Omega$ and $\alpha = 0.99$. The $v_i(t)$ is simulated by sinusoidal waveform with frequency of 100 MHz and amplitude of 0.1 V, the FDTD grid cell size is $\Delta x = \Delta y = \Delta z = 0.25$ mm, $\Delta t = 0.43$ psec with 50,000 time steps, $3\times1\times3$ cells in x, y and z-directions, respectively, 8 CPML layers are used with 5 cells air buffer in every direction. The main goal here is to implement the circuit using the CCCS model shown in Fig. 3 (b) with the new approach and calculate the value of the voltage $v_0(t)$. The results are compared with results generated using analytical solution in Fig. 4 (a). The analytical solution is based on mesh analysis method and it was found that for the values mentioned above, $v_0(t)$ is equal to $64.1732\times v_i(t)$ (BJT circuit with a gain of 64.1732). Figure 4 (a) demonstrates good agreement between analytical solutions and the results of the new approach, which proves the validity of the approach. The error between FDTD and analytical solution is calculated as follows: $\left|\dfrac{V_{FDTD} - V_{Analytical}}{\max\left(V_{Analytical}\right)}\right|\times 100\%$ and plotted in Fig. 4 (b) (the max error is ~3.5%). Furthermore, the same BJT is used to terminate a strip transmission line (TL) as in [15]. Figure 3 (c) shows the BJT circuit with the strip transmission line and ground plane. In this case, $v_i(t)$ is implemented using cosine modulate Gaussian pulse centered at 150 MHz with bandwidth of 250 MHz, and amplitude of 1 V and all other FDTD parameters are kept the same, the transmission line is implemented using $260\times1\times1$ FDTD cells in x, y and z-directions, respectively (6.5 cm long).

From the analytical solution of the BJT circuit, it was found that the voltage gain A_v is 64.1732 as shown above. The time domain results are shown in Fig. 4 (c), the results are compared with the no TL case to show the time delay introduced by the presence of the transmission line. The

computational time using the proposed algorithm is 7.9 minutes, while for the algorithm in [6], it is 8.2 minutes for 50,000 time steps, both were implemented with MATLAB and run using the same computer. In addition to the lower computational time, the proposed algorithm is easier to implement and it could be used for any type of dependent sources application.
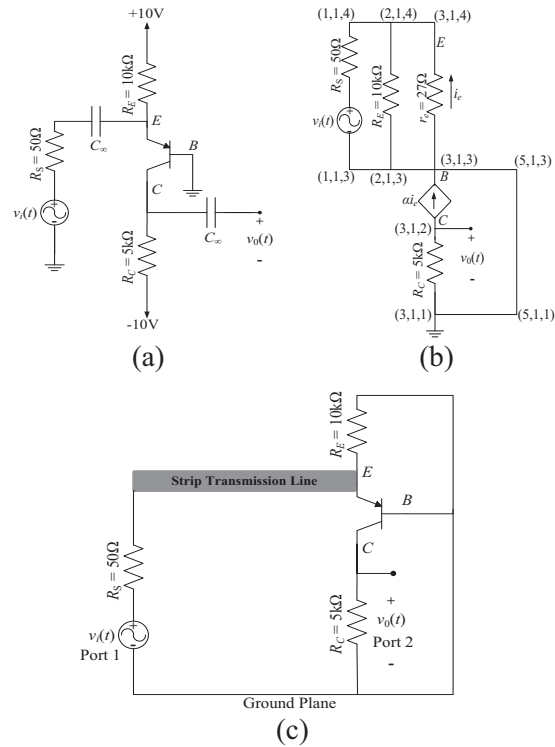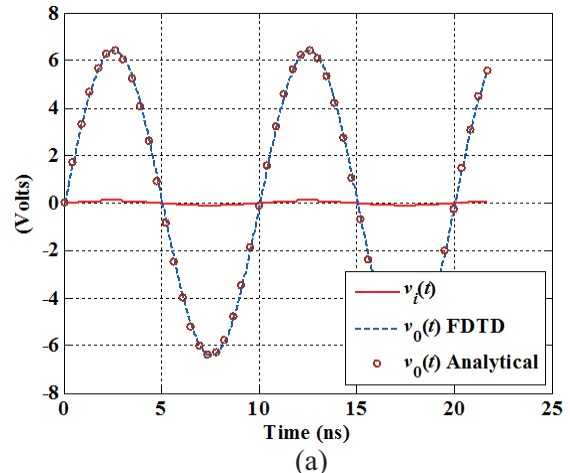

Fig. 3. Test case 2: (a) circuit diagram, (b) the AC analysis equivalent circuit model for BJT using the CCCS T-model with FDTD cell numbers, and (c) AC circuit with integrated transmission line.
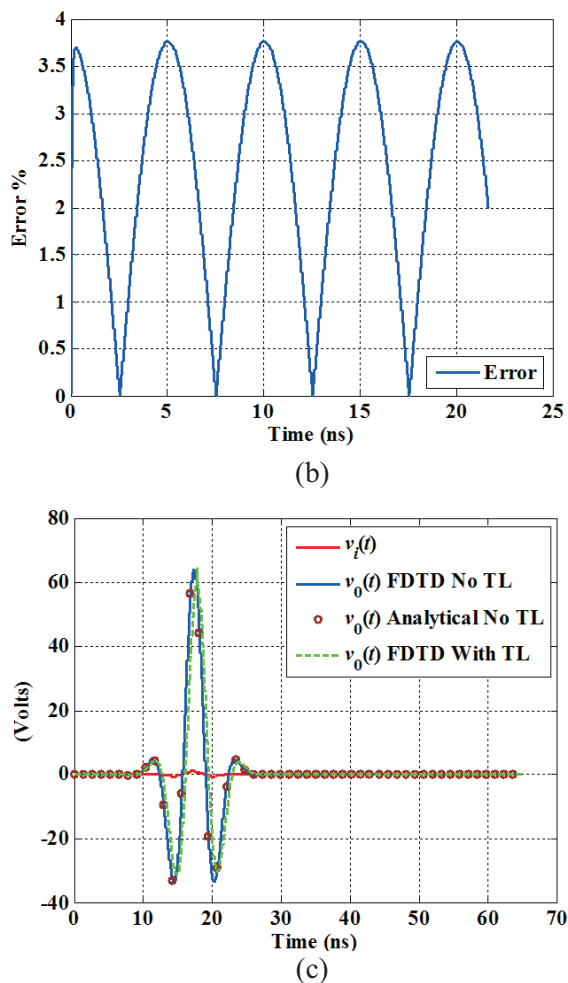

(a)

(b)

(c)

Fig. 4. Time-domain response for test case 2 $v_0(t)$: (a) without TL, (b) shows the relative error for the case without TL, and (c) time-domain response with TL.

IV. CONCLUSION

This paper introduces a new FDTD approach to analyze different types of dependent sources. The approach is simple to implement and efficient in terms of both computational time and memory usage. The approach can be used as a tool to analyze microwave circuits that include dependent sources. In addition, it can be used to implement different non-linear devices using their equivalent circuit models that contain depended sources. The numerical results based on the new approach show very good agreement with results from the analytical solutions, which proves the validity of this approach.

REFERENCES

[1] A. Z. Elsherbeni and V. Demir, "The finite difference time-domain method for electromagnetics: with MATLAB simulations," *SciTech Publishing*, Raleigh, NC, January 2009.

[2] K. ElMahgoub, F. Yang, and A. Z. Elsherbeni, "Scattering analysis of periodic structures using finite-difference time-domain method," *Morgan & Claypool Publishing*, May 2012.

[3] K. ElMahgoub and A. Z. Elsherbeni, "Implementing voltage controlled current source in electromagnetic full-wave simulation using the FDTD method," *International Microwave Symposium Digest (MTT), 2012 IEEE MTT-S*, June 2012.

[4] K. ElMahgoub and A. Z. Elsherbeni, "Implementing current controlled current source in electromagnetic full-wave simulation using the FDTD method," *IEEE International Conference Wireless Information Technology and Systems (ICWITS)*, November 2012.

[5] K. ElMahgoub and A. Z. Elsherbeni, "FDTD implementation of current controlled voltage source," *Middle East Conference on Antennas and Propagation (MECAP)*, December 2012.

[6] M. Piket-May, A. Taflove, and J. Baron, "FD-TD modeling of digital signal propagation in 3-D circuits with passive and active loads," *IEEE Transactions Microwave Theory and Techniques*, vol. 42, no. 8, pp. 1514-1532, August 1994.

[7] F. Kung and H. T. Chuah, "Modeling of bipolar junction transistor in FDTD simulation of printed circuit board," *Progress In Electromagnetics Research, PIER 36*, 179-192, 2002.

[8] F. Kung and H. T. Chuah, "A study on the stability of bipolar-junction-transistor formulation in finite-difference time-domain framework," *IEEE Transactions on Microwave Theory and Techniques*, vol. 53, no. 4, pp. 1189-1196, April 2005.

[9] V. S. Reddy and R. Garg, "An improved extended FDTD formulation for active microwave circuits," *IEEE Transactions on Microwave Theory and Techniques*, vol. 47, no. 9, pp. 1603-1608, September 1999.

[10] O. González, J. A. Pereda, A. Herrera, and A. Vegas, "An extension of the lumped-network FDTD method to linear two-port lumped circuits," *IEEE Transactions on Microwave Theory and Techniques*, vol. 54, no. 7, pp. 3045-3051, July 2006.

[11] C. N. Kuo, V. A. Thomas, S. T. Chew, B. Houshmand, and T. Itoh, "Small signal analysis of active circuits using FDTD algorithm," *IEEE Microwave and Guided Wave Letters*, vol. 5, no. 7,

pp. 216-218, 1995.

[12] C. N. Kuo, R. B. Wu, B. Houshmand, and T. Itoh, "Modeling of microwave active devices using the FDTD analysis based on the voltage-source approach," *IEEE Microwave and Guided Wave Letters*, vol. 6, no. 5, pp. 199-201, May 1996.

[13] C. N. Kuo, B. Houshmand, and T. Itoh, "Full-wave analysis of packaged microwave circuits with active and nonlinear devices: an FDTD approach," *IEEE Transactions on Microwave Theory and Techniques*, vol. 45, no. 5, pp. 819-826, May 1997.

[14] O. El Mrabet and M. Essaaidi, "An efficient algorithm for the global modeling of RF and microwave circuits using a reduced nonlinear lumped network (RNL^{2}N)-FDTD approach," *IEEE Microwave and Wireless Components Letters*, vol. 14, no. 2, pp. 86-88, February 2004.

[15] O. El Mrabet, M. Essaaidi, and M. Drissi, "Global modeling of microwave three terminal active devices using the FDTD method," *IEICE Electronics Express*, vol. 2, no. 2, pp. 43-48, January 2005.

[16] J. Mix, J. Dixon, Z. Popovic, and M. Piket-May, "Incorporating non-linear lumped elements in FDTD: the equivalent source method," *International Journal of Numerical Modeling: Electronic Networks, Devices and Fields*, vol. 12, pp. 157-170, May 1999.

[17] W. Sui, D. A. Christensen, and C. H. Durney, "Extending the two-dimensional FDTD method to hybrid electromagnetic systems with active and passive lumped elements," *IEEE Transactions on Microwave Theory and Techniques*, vol. 40, pp. 724-730, April 1992.

[18] "MATLAB distributed by Mathworks," *www.mathworks.com*.

[19] A. S. Sedra and K. C. Smith, "Microelectronic circuits," fourth edition, *Oxford University Press*, 1997.

Khaled ElMahgoub received his B.Sc. and M.Sc. degrees in Electronics and Electrical Communications Engineering from Cairo University, Egypt, in 2001 and 2006, respectively. He received his Ph.D. degree in Electrical Engineering from the University of Mississippi, USA in 2010. From 2001-2006, he was a Teaching and Research Assistant at Cairo University. From 2007-2010, he was a Teaching and Research Assistant at the University of Mississippi. ElMahgoub is a Research Affiliate with the Auto-ID Labs at MIT. Currently, he is working as Senior Engineer at Trimble Navigation, Cambridge, MA, USA. Possessing over eight years of experience in the industry, he is a Senior Member of the team working in testing and developing RFID technology. Throughout his academic years, he coauthored over 35 technical journals and conference papers. He is a Senior Member of IEEE, Member of ACES and Phi Kappa Phi Honor Society. ElMahgoub is listed in Who's Who in Science and Engineering. He is the recipient of ACES Early Career Award, University of Mississippi scholarship for Ph.D. degree and University of Mississippi graduate school summer assistantship. His current research interests include RFID systems, channel coding, FDTD, antenna design, and numerical techniques for electromagnetics.

Atef Z. Elsherbeni received his Ph.D. degree in Electrical Engineering from Manitoba University, Winnipeg, Manitoba, Canada, in 1987. He joined the University of Mississippi in August 1987 as an Assistant Professor of Electrical Engineering. He advanced to the Associate Professor rank on July 1991, and to the Professor rank in July 1997. At the University of Mississippi, he was also the Director of the School of Engineering CAD Lab from August 2002 to August 2013, the Director of the Center for Applied Electromagnetic Systems Research (CAESR) from July 2011 to August 2013, and the Associate Dean of Engineering for Research and Graduate Programs from 2009 to 2013. He was appointed as Adjunct Professor, with the Department of Electrical Engineering and Computer Science of the L.C. Smith College of Engineering and Computer Science at Syracuse University in January 2004. He spent a sabbatical term in 1996 with the Electrical Engineering Department, University of California at Los Angeles (UCLA), and was a Visiting Professor at Magdeburg University, in Germany during the summer of 2005 and at Tampere University of Technology in Finland during the summer of 2007. He was a Finland Distinguished Professor from 2009 to 2011. Elsherbeni became the Dobelman Distinguished Chair and Professor of Electrical Engineering at the Colorado School of Mines in August 2013. He is a Fellow Member of the Institute of Electrical and Electronics Engineers (IEEE) and a Fellow Member of the Applied Computational Electromagnetic Society (ACES) and the Editor-in-Chief for ACES Journal.